Research Journal of Applied Sciences, Engineering and Technology 7(8): 1603-1611, 2014
DOI:10.19026/rjaset.7.438
ISSN: 2040-7459; e-ISSN: 2040-7467
© 2014 Maxwell Scientific Publication Corp.
Submitted: May 21, 2013 Accepted: June 15, 2013 Published: February 27, 2014

Research Article

Generation of Extensive Moisture Content's Map Using Weighted Moisture Values over Multi-Surface Cover Types

[1]A.A. Hassaballa, [1]A.N. Matori and [2]H.Z.M. Shafri
[1]Department of Civil Engineering, Geoinformatics and Highway Cluster, Universiti Teknologi PETRONAS, UTP, Bandar Sri Iskandar, Malaysia
[2]Department of Civil Engineering, Universiti Putra Malaysia, UPM, Serdang Malaysia

Abstract: The study utilized the Thermal Inertia method (TI) for soil surface moisture (θ) estimation, which is based mainly on two sets of parameters. First, the spatial set, which includes the determination of satellite's surface Temperature (Ts) and the Vegetation Indices (VI). Second, the set of soil parameters, which includes the determination of soil Field Capacity (FC) and the Permanent Wilting Point (PWP) as upper and lower boundaries of the soil water capacity respectively. In this study, MODIS (Aqua/Terra) images were used for estimating the spatial set (Ts and NDVI). Moreover, 3 meteorological stations at 3 different surface cover areas within the study area were selected (Seberang Perak for agricultural land, UTP for multi-cover land and Sitiawan for urban area), then in-situ measurements of FC, PWP, TS and θ were conducted over each station at the time of MODIS satellite overpass. In order to overcome the atmospheric attenuation, the satellite' Ts was rectified by the field measured Ts through regression plots. After that, the satellite θ over the 3 different locations were generated and then validated using the field measured θ. A good agreement was found between the actual and estimated θ, so that, the R^2 over the agricultural area found to be 88%, over the area with multiple surface cover was 81% and over the urban area was 66%. After assuring the validity and the applicability of the used technique, a generalized θ map was generated using weighting factors from three partitions of the surface cover in order to produce an accurate θ map that considers the spectral disparity of variable surface covers within a single pixel.

Keywords: MODIS applications, moisture content, perak tengah and manjung, remote sensing, spectral disparity, thermal inertia method

INTRODUCTION

Surface Soil moisture plays a very significant role in land surface hydrology, so that it controls the portioning of rainfall into run off and infiltration. Along with surface temperature, it affects the depth of planetary boundary layer, circulation/wind patterns (Lanicci *et al*., 1987; Zhang and Crowley, 1989) and regional water energy budgets. Soil moisture tracks the perceptible evaporative water over period of weeks and provides a historical record of atmospheric-land interaction. Moreover, it integrates the land surface hydrology and also acts as an interface between the land surface and the atmosphere. The primary factor in the persistence of dry or wet anomalies over large continental regions during summer is due to the recycling of the water through moisture content, evapotranspiration and precipitation (Bindlish, 2000; Hassaballa and Matori, 2011). Soil moisture can be considered as the most significant boundary condition controlling summer precipitation in the semi-arid zones (Beljaars *et al*., 1996).

On a regional scale, the importance of soil moisture appears in agricultural assessment (crops yield management, irrigation management, etc.), flood and draught control.

Evapotranspiration in turn depends on soil moisture (together with incoming radiation and a host of other meteorological factors) and they help together in determining surface pressure, rainfall and motion (Shukla and Mintz, 1982).

Application of soil moisture: Along with the hydrologic cycle, one of the most important component is soil moisture is because it has an impact on climate change over land and plays the same role over land as sea surface temperature plays over oceans and seas. In some circumstances, it has good potentials of storing the atmospheric signature/energy transferred to it through precipitation (order of months), in turn transferring them back to the atmosphere through evaporation and affecting the climate (Martínez-Fernández and Ceballos, 2003). Soil moisture assists in the determination of the redistribution of rainfall into surface runoff and

Corresponding Author: A.A. Hassaballa, Department of Civil Engineering, Geoinformatics and Highway Cluster, Universiti Teknologi PETRONAS, UTP, Bandar Sri Iskandar, Malaysia
This work is licensed under a Creative Commons Attribution 4.0 International License (URL: http://creativecommons.org/licenses/by/4.0/).

subsurface run off (Delworth and Manabe, 1988; Pauwels *et al*., 2002), so that it controls the portion of energy at the surface as well as the feedback of the water to the atmosphere. Further, it divides the up-willing energy into sensible heat and latent heat fluxes. In addition, soil moisture influences the soil erosion, soil aeration, distribution and growth of vegetation, soil microbial activity, the concentration of toxic substances, the movement of nutrients in the soil to the roots and weather prediction at a local to regional scale (Koster *et al*., 2004). Away from these, there are many other real life applications that soil moisture controls, which make it a very important parameter to measure and study. The following examples have been mentioned due to their influences on human life to some extent:

Drought and flood monitoring: Amount of soil moisture can directly affect the hydrologic drought and flooding because they are closely related to its availability in specific region.

Hydrologic modeling: The assessment of soil water change due to natural and anthropogenic causes is so necessary. Since soil moisture is a main component of water cycle, it will be very helpful to study water cycle processes, precipitation and discharge pattern analysis through knowing the amount of soil water.

Civil engineering: The big structural properties are highly influenced by soil water because it makes soil heavier and softer to hold them sometimes impacts the soil negatively causing landslide at sloppy areas (Hassaballa *et al*., 2013). So, it is so required and important to know and address the moisture amount and variation of the soil water over years. This can assist in aintaining the engineering structures like dams, bridges, roads, etc., that are properly suitable for the soil conditions.

Among the wide range of soil moisture applications in urban, the flood prediction is mentioned which based on the spatial distribution of the saturation of ground soil (Entekhabi *et al*., 1994; Su *et al*., 1995).

Problem statement: Because of the spatial and temporal variability of soil moisture it is considered as a critical hydrological parameter which has direct influences on agriculture, forest ecology, civil engineering, water resources management and crop system modeling as discussed in the previous section. When incorrectly specified, it leads to the mistaken assessment of the other hydrology and energy cycle parameters. Scientists have been trying to recognize the physical relationship among the soil moisture and other ecosystem components (e.g., precipitation, runoff, elevation, soil type, vegetation etc.) through field campaigns, land surface models as well as remote sensing to estimate the soil moisture accurately in a global scale (5).
This study is aiming at:

- Demonstrating the applicability of the Optical/Thermal Infrared remote sensing data and land-use information in soil moisture content (θ) estimation using the Moderate-resolution Imaging

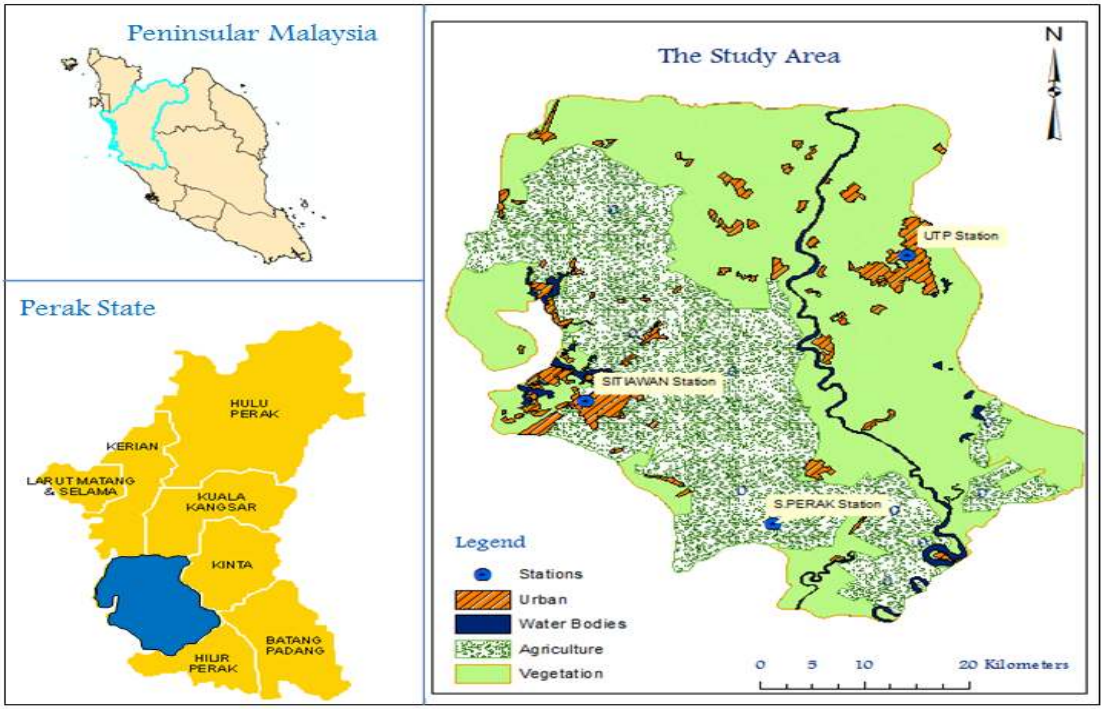

Fig. 1: The study area with classified map for surface cover representation

Spectroradiometer (MODIS) which enjoys high temporal resolution for daily moisture monitoring beside.

- Generating a generalized soil moisture map by correlating three different moisture maps extracted from three dissimilar land covers along the study area in order to simulate the reality of surface cover at the study area.

The study area: Perak Tengah and Manjung are part of Perak state lay between latitude 4°00`- 4°30` N and longitude 100°30`-101°00` E (Fig. 1), with an area of 2,400 km^2. MODIS (Terra and Aqua) images (from June-September 2012) were acquired for θ algorithms generation. Three stations were selected throughout the study area in terms of their variety in environmental and vegetation cover explained as Sitiawan to represent urban area with impervious surfaces, Utp represent a mixed surface cover type and Seberang Perak represents agricultural land.

MATERIALS AND METHODS

Data collection and processing: MODIS Land Surface Temperature and Emissivity (LST/E) product by Aqua MODIS (e.g., MYD11A1 products) and Terra-MODIS (e.g., MOD11A1 products) offered per-pixel temperature and emissivity values every day. Temperatures are produced in Kelvin (K) with a view-angle reliant formula applied to direct observations. MODIS LST algorithm claims producing 1 K accuracy for materials with identified emissivities (Wan, 1999). The view angle details are a part of each LST/E product. Emissivities are estimates that are produced from implementing algorithm output to database information. The LST/E algorithms use MODIS data as input, such as geolocation, radiance, cloud masking, atmospheric temperature, water vapour, snow and land cover. The theoretical foundation in MODIS LST is outlined in detail by Wan (1999). Equally Aqua MODIS and Terra-MODIS LST/E products are supplied daily as a gridded level-3 product in the sinusoidal projection. The availability of daily LST as a MODIS technique is very beneficial for soil moisture scaling research for around two major causes. First, the LST inversion algorithm used by MODIS has been extensively recorded and also the technique is obtainable for assessment. Second, the data is readily obtainable through the internet.

In order to process the acquired AVHRR images for surface temperature extraction, subset area has been delineated surrounding each weather station and any spatial computation performed within each subset area was assumed to represent the average value of the sub area pixels. On the other hand, in-situ measurements of

Fig. 2: Sample station sitiawan (upper) where Ts thermometer (left) and moisture probe (right) are placed

Ts and θ were conducted during the satellite's overpassing time using mini thermometer and a NETRON 740 soil moisture probe, respectively (Fig. 2).

Thermal Inertia (TI) method for moisture estimation: This technique is dependent on the concept that, water bodies possess a higher Thermal Inertia (TI) than dry soils and rocks and demonstrate a lesser diurnal temperature variation. When soil water content raises, thermal inertia relatively raises also, therefore decreasing the diurnal temperature variation range TI could be extracted, starting with the temperature diffusion formula. Many models have been produced using the thermal inertia technique by Xue and Cracknell (1995), Sobrino and El Kharraz (1999) and Mitra and Majumdar (2004) for soil moisture extraction depending on the above mentioned theory however with a little different methods. Among that, (Mitra and Majumdar, 2004) method is considered as essentially the most direct method and comparable to the assumed model by Pegram (2009). Within their method, Apparent Thermal Inertia (ATI, presumed homogeneous layer for TI) is utilized. ATI is inferred through the measurements of spectral surface albedo and also the diurnal temperature range. It signifies the temporal and spatial variation of soil and canopy moisture (Tramutoli *et al*., 2000). The greater ATI, the greater the moisture content of the surface. The basic to derive soil water content is based on the idea that high/low ATI values match maximum/minimum soil moisture contents (Verstraeten *et al*., 2006). By including the Soil Wetness Index (SWI).

The Soil Wetness Index (SWI) for a given day or time (t), which represents relative surface soil moisture, is described as:

$$SWI_{(t)} = \frac{Ts_{\max(i)} - Ts_{(i)}}{Ts_{\max(i)} - Ts_{(\min)}} \quad (1)$$

where,

$Ts_{(i)}$ = The land surface temperature of i-th pixel

$Ts_{(min)}$ = The minimum LST while in the triangle which specifies the wet edge
$Ts_{(max)}$ = The maximum LST for i-th NDVI

To maintain simplicity and consistency in method across various scales, the dry edge was modeled using a linear empirical fit to NDVI:

$$Ts_{\max(i)} = a + bNDVI_{(i)} \quad (2)$$

where,
NDVI = The normalized difference vegetation index of the i^{th} pixel
b = The slope
a = The intercept of the linear dry edge

MODIS's Surface temperature values over study area for the entire period were downloaded directly from web source (http://ladsweb.nascom.nasa.gov/), which is a web interface to the Level 1 and Atmosphere Archive and Distribution System (LAADS). The mission of LAADS is to provide quick and easy access to MODIS Level 1, Atmosphere and Land data products and VIIRS Level 1 and Land data products.

The NDVI measurements were made with a combined red and near-infrared radiometer, developed at the NASA/Goddard Space Flight Center, which measures the reflected radiation in the bands (0.58-0.68 µm) and (0.73-1.1 µm):

$$NDVI = \frac{NIR - RED}{NIR + RED} \quad (3)$$

where NIR and RED are the near-infrared and red reflectance, respectively.

By having the upper (θ_{max}) and lower (θ_{min}) boundaries of volumetric soil moisture within the Surface, the Wetness Index (SWI) over a given day or time could be transformed into a complete estimate of volumetric surface soil moisture (θ_v) making use of the following relationship (Wagner *et al*., 1999):

$$\theta_v = \theta_{\min} + SWI_{(t)}(\theta_{\max} - \theta_{\min}) \quad (4)$$

θ_{max} is the upper limit of θ_v and will undertake values between Field Capacity (FC) and saturated moisture content. Generally, except right after a heavy rainfall event or irrigation θ_{max} could be set similar to FC. For additional practical purposes θ_{max} could be represented as arithmetic mean of FC and maximum retentive capacity (Thapliyal *et al*., 2005; Verstraeten *et al*., 2006). The θ_{min} is the lower limit of θ_v and could be symbolized as Permanent Wilting Point (PWP). These limits are soil type specific. The gap (θ_{max} - θ_{min}) between the two of these boundaries represents Total Water Capacity (TWC) of soil.

In order to determine the upper and lower moisture values which represented in the soil's Field (FC) capacity and the Permanent Wilting Point (PWP) respectively, samples were collected from the soil of

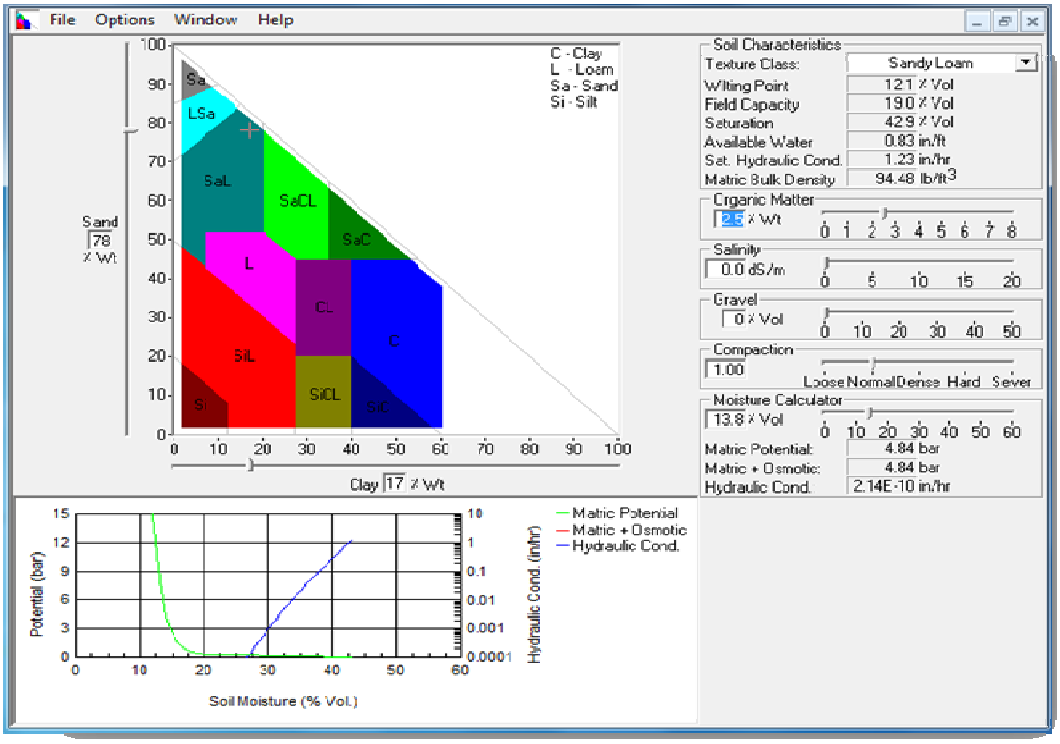

Fig. 3: Soil water characteristics triangle

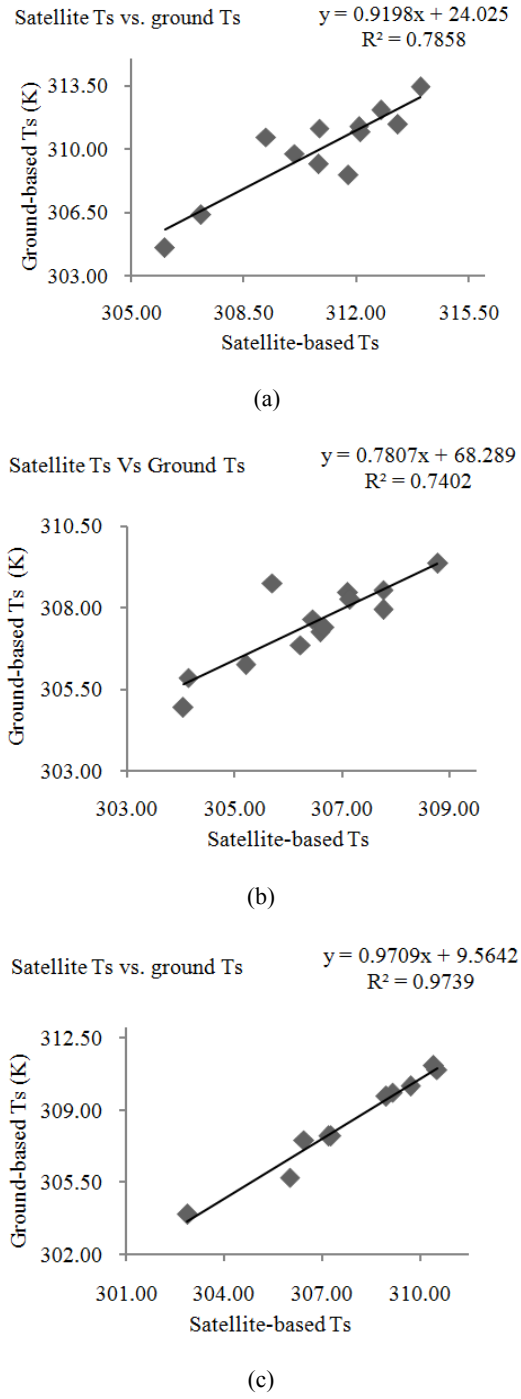

Fig. 4: Simple regression for satellite Ts correction, where (a) Utp, (b) sitiawan and (c) S. perak

each type of the surface cover among the three selected partitions of the study area (full vegetated, urban and multi-cover surfaces). A Particle Size Distribution (PSD) test was applied to the collected samples using (Master-sizer 2000 device) provided by UTP meteorological station. Consequently, soil's structure was classified into the standard classes (sand, silt and clay) with different percentages for surface cover type. Afterward, a hydraulic properties calculator, which is open-source software based on the physical concept of soil water characteristics triangle (Fig. 3) produced by the U.S. Department of Agriculture (USDA), was used to determine the values of (FC) and (PWP) according to the percentage of the soil's components sand and clay.

Temperature correction for soil moisture estimation: In an attempt to estimate a realistic surface moisture value that associated with a perfect surface temperature data, the acquired surface temperatures were related to in-situ measured surface temperatures which their values were recorded concurrently with MODIS overpassing times using sensible hand-held thermometer. Figure 4, shows a simple linear regression relation was used to rectify values of (Ts) then those rectified values (Ts (coreted)) were used in the estimation of SWI instead of (Ts (i)) as in Eq. (1).

RESULTS

Table 1 below demonstrates the resultant values for θ_{max} and θ_{min} which are represented by the field capacity and also the permanent wilting point respectively. FC and PWP were obtained from the soil water characteristics triangle. The utilized strategy was that, the higher Ts value within each subset area of an image was applied to represent $Ts_{max(i)}$ after which plotted up against the average value of the respective $NDVI_{(i)}$ from the same image. Identically, $Ts_{min(i)}$ was picked as the least $Ts_{(i)}$ value within the image subset, while pixel-based Ts was represented by the average value of the subset area. All these were carried out, with regards to develop simulated point measurements of soil moisture from the image pixels so that we can produce a realistic and well validated moisture values.

Moisture generation and validation: According to Eq. (4), volumetric moisture content was extracted for 12 daily MODIS (Aqua/Terra) acquired images accompanied with in-situ measurements of moisture content over Utp and 14 images for Sitiawan stations as well as 11 images over Seberang Perak area. The produced satellite's moisture values which are in term of point measurements, were validated using the moisture measurements conducted in-situ in forms of correlation relationship as a step to examine the accuracy of moisture scaling in assessing soil moisture. Table 2 below shows the statistical characteristics and the significance of the relationship between moisture conducted at field and the satellite's estimated moisture with rectified surface temperature.

Derivation of generalized moisture map: The concept of the generalized map derivation is based fundamentally on the estimation of a pixel-based

moisture content value, within which, variable surface cover types share the spectral signatures to generate the moisture.

Based on that, weightage of each of the three different cover types was determined and imposed in the generalized map formation. Firstly, satellite's surface moisture maps were generated using a pixel-based SWI in addition to the FC and PWP from each of the three stations, in which, the moisture map at pixel (i) level using the moisture boundaries over Utp station took the value of θ_{UTP_i}, same tasks went with the moisture images generated over Sitiawan and Seberang perak which represented by θ_{SITI_i} and θ_{SP_i} respectively. The total moisture map of the pixel based image was calculated as a summation of the three moisture values for each pixel (θ_{SUM_i}) then, the fraction (F_{R_i}) of station's moisture share within the pixel was calculated as a percentage of the pixel moisture value of the particular station to the total moisture at the pixel. Eq. (5) to (12) below describe mathematically the steps towards the generalized moisture estimation over the study area:

Table 1: The resultant moisture limits

Station	θ_{max} (FC)	θ_{min} (PWP)
UTP	0.23	0.12
Sitiawan	0.27	0.17
Seberang perak	0.23	0.11

Table 2: Significance of the relationships

		In-situ measured moisture content		
		UTP	Sitiawan	S. perak
Corrected-Ts moisture content with SWI generated from (NDVI) -UTP	P. correlation	0.811		
	Sig. (2-tailed)	0.001		
	N*	12		
Corrected-Ts moisture content with SWI generated from (NDVI) -sitiawan	P. correlation		0.663	
	Sig. (2-tailed)		0.014	
	N		13	
Corrected-Ts moisture content with SWI generated from (NDVI) -S. perak	P. correlation			0.88700
	Sig. (2-tailed)			0.00028
	N			11

N*: Number of satellite's images

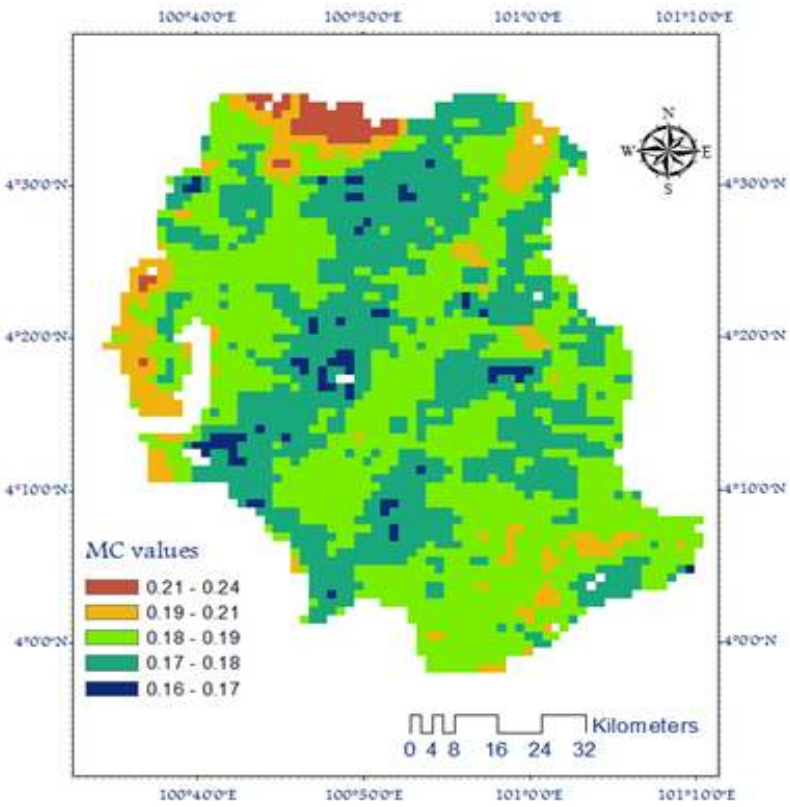

Fig. 5: Moisture content generalized map from corrected-Ts

$$\theta_{SUM_i} = \sum_{i=1}^{n} (\theta_{UTP_i}, \theta_{SITI_i}, \theta_{SP_i}) \quad (5)$$

$$Fr_{UTP_i} = \theta_{SITI_i} \Big/ \theta_{SUM_i} \quad (6)$$

$$Fr_{SITI_i} = \theta_{UTP_i} \Big/ \theta_{SUM_i} \quad (7)$$

$$Fr_{SP_i} = \theta_{SP_i} \Big/ \theta_{SUM_i} \quad (8)$$

The weight age (W_i) of each surface cover type for the single pixel was determined by applying the fraction of each station to the corresponding full moisture pixel which was generated by own boundaries (FC and PWP). Finally, the generalized moisture (θ_i) for each image pixel was calculated as a summation of the three different weightages of pixel's moisture:

$$W_{UTP_i} = Fr_{UTP_i} \times \theta_{UTP_i} \quad (9)$$

$$W_{SITI_i} = Fr_{SITI_i} \times \theta_{SITI_i} \quad (10)$$

$$W_{SP_i} = Fr_{SP_i} \times \theta_{SP_i} \quad (11)$$

$$\theta_i = W_{UTP_i} + W_{SITI_i} + W_{SP_i} \quad (12)$$

Figure 5 shows the moisture content map extracted as a result of the correlation between the 3 different land covers tested earlier in the study which are: the urban areas represented by Sitiawan station, the agricultural area represented by Seberang Perak paddy field and the multiple surface cover represented by Utp station. The image was acquired in June 12, 2009 from MODIS Terra sensor with spatial resolution of 1 km^2.

DISCUSSION

The moisture validation produced a reasonable connection with a high significance between moisture estimated over the agricultural land of Seberang Perak and its in-situ measurements is exist, this could be attributed to the uniformity of the vegetation cover represented in the cultivated crops the which tend to reduce the Ts values producing a relatively high SWI over the entire area. On the other hand, a moderate relationship was found between the two sets of moisture content over Sitiawan area (built up area), this is certainly because soils over the urban areas get impervious due to compaction activities asphalt embedding which lead to evaporate the any water that kept at the surface preventing soil from holding it. In addition to that, the latent heat of vaporization is relatively higher over the urban areas as a normal result of the high temperature and emissivities generated by constructions, street engines and roofing materials, all these lead to a drastic reduction in surface moisture. Away from that, the third part which is occupied by partial vegetation cover shared with scattered patches of agricultural fields beside some residential areas produced a significant correlation along the distributed surface covers.

With the large ground cover of every AVHRR or MODIS pixel (almost 1 km^2), the assumption is that there is non-homogeneity throughout each area equivalent to a satellite measurement. Mainly, every single area could be a mixture of vegetation, wet soil and dry soil. The surface moisture detected by satellite can also be thought to be a combination of the high, moderate and moisture values in correspondence to the surface cover type.

The essential concern in employing this technique is to locate three distinctive land use/cover types (i.e., vegetation, multi-cover land and dry land) which are homogeneous and large enough to be recognized by satellite sensor and, that the moisture content could be estimated taking into account the influence of the dry surfaces over the urban areas, the green homogenous cover over the agricultural field and forests as well as the land patch shared with scattered vegetation and impervious surface. All these feature are most likely exist within a single pixel of MODIS or AVHRR image, because of that, the generalization of moisture such a way, was assumed to simulate and represent the typical surface moisture for the particular image pixel with the advantage of extracting this value for a quite pig region covered by a single scene.

CONCLUSION

The assumption is that, moisture availability ranges linearly from the dry edge to the wet edge. This could be in complete agreement with the understanding of LST-NDVI space (Carlson *et al*., 1994; Stisen *et al*., 2008). The Soil Wetness Index (SWI) for the study area, which represents relative surface soil moisture, was determined based on the averaged-pixel's Ts and NDVI in order to simulate the point measurement of the moisture content over both different types of the study area. Further, by having the upper (θ_{max}) and lower (θ_{min}) boundaries of volumetric soil moisture within the Surface, the Wetness Index (SWI) over the given area has been transformed into a complete estimate of volumetric surface soil moisture (θ_v) making use of the relationship produced by Wagner *et al*. (1999).

The satellite rectified-Ts obtained reasonable results in surface moisture content estimation, particularly over agricultural area and areas with a homogeneous cover, so that, the produced correlation

coefficient between the satellite's corrected Ts and the measured Ts *in-situ* has the highest values compared to Ts generated by the rest. A surface moisture content algorithm was validated spatially by comparing the satellite's moisture content to in-situ measured ones.

Finally, the generalized moisture map was calculated upon a pixel-base weighting. So that, the participation of each land surface cover within the image pixel could be imposed in a try to surpass the limitation of the coarse resolution that justifies the limited usage of MODIS images as well as the satellites those have typical resolutions. In addition, the technique managed to express the status of moisture content at the surface taking into account the variable soil textures and their holding capacities through encompassing FC and PWP of the soil profiles into a single pixel. This appears to be more sensitive technique that utilizing the thermal characteristics, vegetation cover as well as the physical structure of soil in assessing the moisture content, while most of other optical technique are dependent of temperature and vegetation cover allocation.

REFERENCES

Beljaars, A.C.M., P. Viterbo, M.J. Miller and A.K. Betts, 1996. The anomalous rainfall over the United States during July 1993: Sensitivity to land surface parameterization and soil moisture anomalies. Monthly Weather Rev., 124: 362-383.

Bindlish, R., 2000. Active and passive microwave remote sensing of soil moisture. Ph.D. Thesis, The Pennsylvania State University.

Carlson, T.N., R.R. Gillies and E.M. Perry, 1994. A method to make use of thermal infrared temperature and NDVI measurements to infer surface soil water content and fractional vegetation cover. Remote Sens. Rev., 9(1-2): 161-173.

Delworth, T. and S. Manabe, 1988. The influence of potential evaporation on the variabilities of simulated soil wetness and climate. J. Climate, 1: 523-547.

Entekhabi, D., H. Nakamura and E.G. Njoku, 1994. Solving the inverse problem for soil moisture and temperature profiles by sequential assimilation of multifrequency remotely sensed observations. IEEE T. Geosci. Remote Sens., 32: 438-448.

Hassaballa, A.A. and A.B. Matori, 2011. Study on surface moisture content, vegetation cover and air temperature based on NOAA/AVHRR surface temperatures and field measurements. Proceeding of National Postgraduate Conference (NPC), Kuala Lumpur, pp: 1-5.

Hassaballa, A.A., O.F. Althuwaynee and B. Pradhan, 2013. Extraction of soil moisture from RADARSAT-1 and its role in the formation of the 6 December 2008 landslide at Bukit Antarabangsa, Kuala Lumpur. Arab. J. Geosci., 1-10: 1866-7511.

Koster, R.D., M.J. Suarez, P. Liu, U. Jambor, A. Berg, M. Kistler, R. Reichle, M. Rodell and J. Famiglietti, 2004. Realistic initialization of land surface states: Impacts on subseasonal forecast skill. J. Hydrometeorol., 5: 1049-1063.

Lanicci, J.M., T.N. Carlson and T.T. Warner, 1987. Sensitivity of the Great Plains severe-storm environment to soil-moisture distribution. Monthly Weather Rev., 115: 2660-2673.

Martínez-Fernández, J. and A. Ceballos, 2003. Temporal stability of soil moisture in a large-field experiment in Spain. Soil Sci. Soc. Am. J., 67: 1647-1656.

Mitra, D.S. and T.J. Majumdar, 2004. Thermal inertia mapping over the Brahmaputra basin, India using NOAA-AVHRR data and its possible geological applications. Int. J. Remote Sens., 25: 3245-3260.

Pauwels, V., R. Hoeben, N.E.C. Verhoest, F.P. De Troch and P.A. Troch, 2002. Improvement of TOPLATS-based discharge predictions through assimilation of ERS-based remotely sensed soil moisture values. Hydrol. Process., 16: 995-1013.

Pegram, G.G.S., 2009. A nested multisite daily rainfall stochastic generation model. J. Hydrol., 371: 142-153.

Shukla, J. and Y. Mintz, 1982. Influence of land-surface evapotranspiration on the Earth's climate. Science, 215: 1498-1501.

Sobrino, J.A. and M.H. El Kharraz, 1999. Combining afternoon and morning NOAA satellites for thermal inertia estimation 2: Methodology and application. J. Geophys. Res., 104: 9455-9465.

Stisen, S., I. Sandholt, A. Nørgaard, R. Fensholt and K.H. Jensen, 2008. Combining the triangle method with thermal inertia to estimate regional evapotranspiration: Applied to MSG-SEVIRI data in the senegal river basin. Remote Sens. Environ., 112: 1242-1255.

Su, Z., P.A. Troch, F.P. De Troch, L. Nochtergale and B. Cosyn, 1995. Preliminary results of soil moisture retrieval from ESAR (EMAC 94) and ERS-1/SAR, Part II: Soil Moisture Retrieval. Proceedings of the 2nd Workshop on Hydrological and Microwave Scattering Modelling for Spatial and Temporal Soil Moisture Mapping from ERS-1 and JERS-1SAR Data and Macroscale Hydrologic Modeling (EV5V-CT94-0446). Institute National de la Recherche Agronomique, Unité de Science du Sol et de Bioclimatologie, France, pp: 7-19.

Thapliyal, P.K., P.K. Pal, M.S. Narayanan and J. Srinivasan, 2005. Development of a time series-based methodology for estimation of large-area soil wetness over India using IRS-P4 microwave radiometer data. J. Appl. Meteorol., 44: 127-143.

Tramutoli, V., P. Claps, M. Marella, N. Pergola and C. Sileo, 2000. Feasibility of hydrological application of thermal inertia from remote sensing. Proceeding of 2nd Plinius Conference, pp: 16-18.

Verstraeten, W.W., F. Veroustraete, C.J. Van Der Sande, I. Grootaers and J. Feyen, 2006. Soil moisture retrieval using thermal inertia, determined with visible and thermal spaceborne data, validated for European forests. Remote Sensing Environ., 101: 299-314.

Wagner, W., G. Lemoine and H. Rott, 1999. A method for estimating soil moisture from ERS scatterometer and soil data. Remote Sensing Environ., 70: 191-207.

Wan, Z., 1999. MODIS Land-Surface Temperature Algorithm Theoretical Basis Document (LST ATBD). Institute for Computational Earth System Science, Santa Barbara, 75.

Xue, Y. and A.P. Cracknell, 1995. Advanced thermal inertia modelling. Remote Sensing, 16: 431-446.

Zhang, J. and T.J. Crowley, 1989. Historical climate records in China and reconstruction of past climates. J. Climate, 2: 833-849.